




The interaction of insoluble Amyloid- β with soluble Amyloid- β dimers decreases Amyloid- β plaque numbers

Else F. van Gerresheim¹ | Arne Herring² | Lothar Gremer^{3,4,5}  |
Andreas Müller-Schiffmann¹ | Kathy Keyvani²  | Carsten Korth¹ 

¹Department of Neuropathology, Heinrich Heine University Düsseldorf, Düsseldorf, Germany

²Institute of Neuropathology, University of Duisburg-Essen, Essen, Germany

³Institute of Physical Biology, Heinrich Heine University Düsseldorf, Düsseldorf, Germany

⁴Institute of Biological Information Processing (IBI-7) and JuStruct, Jülich Center for Structural Biology, Research Centre Jülich, Jülich, Germany

⁵Research Center for Molecular Mechanisms of Aging and Age-Related Diseases, Moscow Institute of Physics and Technology (State University), Dolgoprudny, Russia

Correspondence

Carsten Korth, Department of Neuropathology, Heinrich Heine University Düsseldorf, Moorenstrasse 5, 40225 Düsseldorf, Germany.
Email: ckorth@hhu.de

Funding information

Deutsche Forschungsgemeinschaft, Grant/Award Number: KO 1679/10-1; BMBF, Grant/Award Number: 01GQ1422; Russian Science Foundation, Grant/Award Number: 20-64-46027

Abstract

Objectives: The heterogeneity of Amyloid-beta ($A\beta$) plaque load in patients with Alzheimer's disease (AD) has puzzled neuropathology. Since brain $A\beta$ plaque load does not correlate with cognitive decline, neurotoxic soluble $A\beta$ oligomers have been championed as disease-causing agents in early AD. So far, investigating molecular interactions between soluble oligomeric $A\beta$ and insoluble $A\beta$ *in vivo* has been difficult because of the abundance of $A\beta$ oligomer species and the kinetic equilibrium in which they coexist. Here, we investigated whether $A\beta$ plaque heterogeneity relates to interactions of different $A\beta$ conformers.

Materials and Methods: We took advantage of transgenic mice that generate exclusively $A\beta$ dimers (tgDimer mice) but do not develop $A\beta$ plaques or neuroinflammation during their lifetime, crossed them to the transgenic CRND8 mice that develop plaques after 90 days and measured $A\beta$ plaque load using immunohistochemical and biochemical assays. Furthermore, we performed *in vitro* thioflavin T (ThT) aggregation assays titrating synthetic $A\beta_{42}$ -S8C dimers into fibril-forming synthetic $A\beta_{42}$.

Results: We observed a lower number of $A\beta$ plaques in the brain of double transgenic mice compared to tgCRND8 mice alone while the average plaque size remained unaltered. Corroborating these *in vivo* findings, synthetic $A\beta$ -S8C dimers inhibited fibril formation of wild-type $A\beta$ also *in vitro*, seen by an increased half-time in the ThT assay.

Conclusions: Our study indicates that $A\beta$ dimers directly interfere with $A\beta$ fibril formation *in vivo* and *in vitro*. The variable interaction of $A\beta$ dimers with insoluble $A\beta$ seeds could thus contribute to the heterogeneity of $A\beta$ plaque load in AD patients.

KEYWORDS

Amyloid-beta, Alzheimer's disease, dimer, fibril formation

Abbreviations: AD, Alzheimer's disease; APP, Amyloid precursor protein; $A\beta$, Amyloid beta; EDTA, Ethylenediaminetetraacetic Acid; ELISA, Enzyme-Linked Immunosorbent Assay; gDNA, Genomic DNA; haPrP, Syrian hamster prion gene; HFIF, Hexafluoroisopropanol; qPCR, Quantitative real-time Polymerase Chain Reaction; RF, Rigid Fibril; RP-HPLC, Reverse-Phase High-Performance Liquid Chromatography; SDS, Sodium Dodecyl Sulphate; TBS, Tris-Buffered Saline; TBST, Tris-Buffered Saline/0.025% Tween 20; ThT, Thioflavin T.

This is an open access article under the terms of the Creative Commons Attribution-NonCommercial-NoDerivs License, which permits use and distribution in any medium, provided the original work is properly cited, the use is non-commercial and no modifications or adaptations are made.

© 2020 The Authors. *Neuropathology and Applied Neurobiology* published by John Wiley & Sons Ltd on behalf of British Neuropathological Society.

INTRODUCTION

Amyloid-beta ($A\beta$) plaque load in patients with Alzheimer's disease (AD) is heterogeneous and often does not correlate with cognitive deficits (1–4). This has remained a conundrum, as $A\beta$ plaques have been a defining feature of AD since its inception. To this end, $A\beta$ oligomers and tau fibrillization are better correlates of failing cognition (5). Accordingly, the amyloid cascade hypothesis of AD, claiming that $A\beta$ multimerization is causal in the neuropathology of AD, has consequently shifted to $A\beta$ oligomers as causative agents in early AD (5).

However, the term $A\beta$ “oligomer”, at this stage, is poorly defined and comprises anything from dimers to 24-mers (6), each with potentially different and possibly even opposing effects. For example, $A\beta$ oligomers have been proposed to be predecessors of $A\beta$ plaques (7), to be sequestered by $A\beta$ plaques as a protective mechanism (8), but also to be shed from plaques, which act as a reservoir (9). The ongoing problem with studying the effects of different species of insoluble/multimeric and soluble/oligomeric species of $A\beta$ in brains, cellular systems or cell-free systems is the existence of a kinetic equilibrium between different species, that is, the inability to investigate exclusive $A\beta$ species at defined concentrations without permanently ongoing dynamic changes in their multimerization or conformation. For these reasons, stabilized dimeric $A\beta$ variants have been generated, either by introducing intermolecular disulfide bridges (10,11) or by linking two $A\beta$ peptides head to tail via a flexible glycine–serine-rich linker (12).

We previously generated a disulfide-stabilized $A\beta$ dimer via replacing a serine at position 8 of the $A\beta$ domain with a cysteine. This mutant allowed preparations of synthetic $A\beta$ -S8C dimers as well as the generation of naturally secreted $A\beta$ -S8C dimers after processing of a corresponding active amyloid precursor protein (APP) mutant in cell culture and in an *in vivo* mouse model termed tgDimer mouse (13,14). We took advantage of these tgDimer mice that express human APP₇₅₁ K670 N / M671L (Swedish) / S679C under control of the Thy1 promoter and in which exclusively $A\beta$ -S8C dimers are generated but no other $A\beta$ species including monomers (14). TgDimer mice are remarkable since they express no insoluble $A\beta$, hence, do not develop $A\beta$ plaques, astrogliosis or neuroinflammation during their lifetime. Yet they show learning and memory deficits as well as anxiety and despair-related behaviours with aberrant serotonin and acetylcholine levels and thus reflect features of early AD (14,15).

To investigate how $A\beta$ plaque heterogeneity may relate to interactions of different $A\beta$ conformers, we analysed the aggregation propensity of $A\beta$ -S8C dimers in the presence of wild-type $A\beta$ seeds by crossing the tgDimer mouse with the transgenic CRND8 (tgCRND8) mouse, a mouse line expressing human APP₆₉₅ K670 N / M671L (Swedish) / V717F (Indiana) under control of the Syrian hamster (ha) PrP promoter (16). We investigated plaque formation in 3- and 5-month-old tgCRND8/tgDimer mouse brains and compared them to tgCRND8 brains of same age. In order to simulate these $A\beta$ interactions *in vitro*, we used the thioflavin T (ThT) assay, where we

added varying amounts of stabilized synthetic $A\beta_{42}$ -S8C dimers to wild-type $A\beta_{42}$.

Our data suggest that the presence of $A\beta$ -S8C inhibits $A\beta$ plaque seeding, although plaque size remained the same when compared to tgCRND8 mice suggesting an inhibitory effect of $A\beta$ -S8C dimers on amyloid fibril formation. By adding $A\beta_{42}$ -S8C to the aggregation-prone wild-type $A\beta_{42}$ *in vitro*, we observed an increased time of seeding onset supporting the idea that $A\beta$ dimers inhibit fibril formation but not growth.

MATERIALS AND METHODS

Animals

TgCRND8 mice express human APP₆₉₅ with the familial Swedish (K670 N / M671L) and Indiana (V717F) mutations under control of the Syrian hamster prion gene (haPrP) promoter, and have been extensively characterized before (16). TgDimer mice express human APP₇₅₁ with the Swedish mutation and the dimer mutation within the $A\beta$ domain (S679C) that generates $A\beta$ -S8C dimers. The mice used here (tgCRND8/tgDimer) were hemizygous for APP carrying the Swedish and Indiana mutation (from CRND8) and hemizygous for APP carrying the Swedish and $A\beta$ -S8C mutation (from tgDimer). Animal experiments were performed in accordance with the German Animal Protection Law and were authorized by local authorities (LANUV NRW, Germany). Mice were housed under standard laboratory conditions with lights on from 7 a.m. to 7 p.m. and with water and food provided *ad libitum*.

Antibodies

Iba1 antibody (EPR16588) was bought from Abcam. GFAP-specific antibody (Z0334) and the $A\beta$ antibodies 6F/3D, M0872, were purchased from DAKO. IC16 and CT15 antibodies were described elsewhere (17,18) and used in combination with secondary goat anti-mouse or goat anti-rabbit POD-linked antibodies (ThermoFisher 1:25,000). In addition, anti-Actin (A2066) and anti-Tubulin (T9026) antibodies were purchased from Sigma. Additionally, goat anti-mouse IRDye 680RD and goat anti-rabbit 800CW (from LI-COR) were used as secondary antibodies.

Brain tissue preparation

At postnatal day 90 (P90) and 150 (P150), tgCRND8, tgCRND8/tgDimer and tgDimer mice were euthanized and their brains removed. One hemisphere was fixed overnight in 4% buffered formaldehyde, followed by paraffin embedding. Afterwards, the hemisphere was cut into 10- μ m-thick coronal sections. The other hemisphere was snap-frozen in liquid N₂ before genomic DNA (gDNA) was extracted from homogenized tissue of this hemisphere

to quantify gene expression by quantitative real-time polymerase chain reaction (qPCR).

Immunohistochemistry

A β plaques were visualized by immunohistochemistry using the 6F/3D antibody at a dilution of 1:100 and stereologically quantified in 8 coronal brain sections (with 100 μ m interspace between sections) per animal at 200 \times magnification. A β plaque number (n/mm²) was determined in an unbiased manner by an area fraction fractionator (counting frame 300 \times 300 μ m, grid size 425 \times 425 μ m for both probes). The average plaque size (μ m²) was calculated by dividing the total A β plaque-positive area by the total plaque number. Absolute values were related to the investigated area. A Nikon 80i microscope, a colour digital camera (3/4" chip, 36-bit colour, DV-20, MicroBrightField) and MicroBrightField software Stereo Investigator 11 were used.

Quantitative real-time RT-PCR

gDNA was isolated using a lysis buffer containing EDTA and 1% SDS from the 10% brain homogenate samples. Expression levels of the APP transgene in CRND8 were determined using the following primers: haPrP-5'-3' TGGCTAGTCAGGGCTTTGTT (forward primer) and haPrP-5'-3' TGGGAGGCTGTTTCTTAGGG (reverse primer) both targeting the promoter region of haPrP.

The APP (A β -S8C) transgene was quantified with: pTS-CAPPswe3600-5'-3' CTGCCTCTCTGCCTCTCTGC (forward primer) and APPseq3R-5'-3' CACAGAACATGGCAATCTGG (reverse primer) to target the Thy1 promoter region. Raw Ct values were used to calculate relative expression levels of target genes, after normalization to the internal control gene β -actin.

Four-step ultracentrifugation fractionation

The amount of insoluble A β in tgCRND8 and in tgCRND8/tgDimer mouse brains was determined by performing a four-step ultracentrifugation as described previously (19). Briefly, 100 μ L of 10% homogenates Tris-buffered saline (TBS) were centrifuged at 100,000 \times g at for 1 h at 4°C. The supernatants (soluble free A β) were harvested and the pellets were resuspended in 100 μ L TBS/1% Triton TX-100 by sonication. After centrifugation at 100,000 \times g at 4°C for 1 h, the supernatants (membrane bound A β) were taken and the precipitates dissolved in 100 μ L TBS/2% SDS by sonication. After centrifugation at 100,000 \times g at room temperature, the supernatants (protein bound A β) were harvested and the precipitates were finally dissolved in 100 μ L of 70% formic acid (plaque-associated insoluble A β) before being centrifuged again for 1 h at 100,000 \times g at room temperature. The first three supernatants were diluted 20-fold in TBS and the formic acid

fraction was neutralized by adding 20 volumes of 1 M unbuffered Tris solution.

A β ELISA

Insoluble A β_{40} and A β_{42} were extracted from brain homogenates after four-step fractionation with 70% formic acid and quantified using the A β_{40} or A β_{42} kit from Invitrogen (Invitrogen; KHB3481 and KHB3441) according to the manufacturer's protocol. A β concentrations were calculated relative to the monomer concentration of the standard and are indicated as pmol/g protein. A β levels were normalized using the protein concentration measured with the DC™ (detergent compatible) protein assay (Bio-Rad).

Western Blot

For visualization of Iba1 and GFAP, 30 and 20 g of 10% whole-brain homogenates respectively in 100 mM Tris HCl pH 7.5, 140 mM NaCl and 3 mM KCl (TBS) containing Complete protease inhibitor cocktail (Roche) were separated on a NuPAGE 4–12% Bis-Tris Gel (Life technologies), using NuPAGE Sample buffer with addition of 2% (v/v) of β -mercaptoethanol and transferred to a 0.2 μ m nitrocellulose membrane. The membranes were blocked with PBS/5% skimmed milk and incubated with either primary antibodies against Iba1 (1:2,000) or GFAP (1:2,500) and actin (1:5,000) or tubulin (1:5,000) diluted in TBS/0.025% Tween20 (TBST). After 3x washing with TBST and incubation with appropriate secondary antibodies, signals were quantified by densitometric analysis using the Odyssey infrared imaging system (LI-COR).

For A β species visualization, 10% brain homogenates and the fractions derived from four-step fractionation were incubated with IC16-coupled NHS agarose beads (13). After washing with PBS, bound APP/A β was eluted with NuPAGE sample buffer/2% β -mercaptoethanol, and afterwards separated on a 4–12% Bis-Tris Gel. The membrane was boiled for 10 min in PBS after separation, before blocking with PBS/5% skimmed milk. The membrane was incubated with the antibody 4G8 against A β (1:500) diluted in TBST respectively. After washing three times with TBST and incubation with secondary horseradish peroxidase conjugated (POD) antibody, signals were detected with SuperSignal™ West Pico PLUS Chemiluminescent Substrate (ThermoFisher). The same blot was washed and incubated with CT15 (1:3,500) in TBST for APP fragment detection, and signals were visualized using the LI-COR system.

A β_{42} and A β_{42} -S8C dimer preparation

A β_{42} was purchased from Bachem, A β_{42} -S8C was synthesized by JPT Peptide Technologies. Both were treated with hexafluoroisopropanol (HFIP) and lyophilized before use. Subsequently, A β_{42} -S8C was dissolved in 50 mM HEPES NaOH pH 7.6 and incubated for at least 4 h

to complete dimerization. Thereafter, the dimerized fraction was purified by reverse-phase high-performance liquid chromatography (RP-HPLC) on a Zorbax 300 SB-C8 column (4.6 mm x 250 mm) connected to an Agilent 1260 system and lyophilized again. Another HFIP treatment ensured the presence of pure non-aggregated A β ₄₂-S8C dimers. Immediately before use, the A β proteins were dissolved in 50 mM HEPES NaOH pH 7.6 buffer to a stock concentration of 20 μ M.

Thioflavin T (ThT) assay

Five μ M A β ₄₂ were mixed with varying amounts of A β ₄₂-S8C dimers (between 0.25 and 2.5 μ M) in 50 mM HEPES NaOH pH 7.6 containing 10 μ M ThT (Abcam) up to a volume of 55 μ L into wells of a half area black/clear flat bottom polystyrene 96-wells plate (Corning). On the same plate, varying amounts of A β ₄₂-S8C dimers in 50 mM HEPES NaOH pH 7.6 were mixed with 10 μ M ThT. The ThT fluorescence of A β ₄₂-S8C dimers was later subtracted from the ThT fluorescence obtained from 5 μ M A β ₄₂ mixed with A β ₄₂-S8C dimers. The outermost wells of the plate were filled with buffer and ThT

only, in order to reduce artefactual measurements on marginal rows and columns. ThT fluorescence was measured using a FluoStar plate reader (BMG Labtech) at 30°C with orbital shaking at 700 rpm for at least 24 h. ThT fluorescence was excited at 448 nm and emission collected at 482 nm.

Statistical analysis

Data are depicted as means \pm SEM. Normal distribution of the data sets was tested by Pearson's normality test. Mann-Whitney Test was applied for the analyses of two groups, unless stated otherwise. Differences were considered significant at $p < 0.05$. All tests were performed utilizing GraphPad Prism 8.4.2.

RESULTS

APP transgene expression levels of tgDimer, tgCRND8 and tgCRND8/tgDimer mice were measured by qPCR. The expression

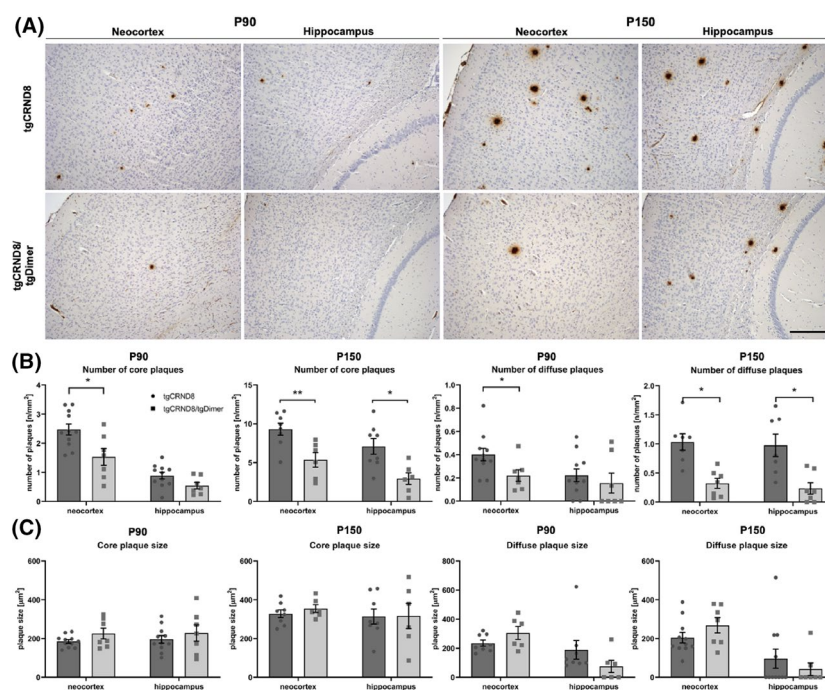


FIGURE 1 Morphological and biochemical differences between tgCRND8 (P90, $n = 11$; P150, $n = 8$) and tgCRND8/tgDimer (P90, $n = 7$; P150, $n = 6$) mice. Core plaques were defined as compact dense plaques, whereas diffuse plaques were defined as an amorphous structure, without a clear border. Mann-Whitney tests were used to test for statistical significance. (A) Representative immunohistochemical images of the neocortex and hippocampus for A β are presented for tgCRND8 and tgCRND8/tgDimer mice at P90 and P150. At P90, few plaques are detected in both genotypes, whereas at P150 more A β deposits are detected in the tgCRND8 mouse compared to the tgCRND8/tgDimer mouse. Antibody 6F/3D. Scale bar = 200 μ m. (B) There is a significantly higher number of core plaques in the neocortex of the tgCRND8 mice (2.5 ± 0.2) compared to the tgCRND8/tgDimer mice (1.5 ± 0.3 ; $p = 0.0268$) at P90. The number of core plaques in the neocortex and hippocampus is significantly higher in tgCRND8 mice (9.3 ± 0.8 and 7.1 ± 1.0) versus tgCRND8/tgDimer mice at P150 (5.4 ± 0.9 and 2.9 ± 0.8 ; $p = 0.0127$, $p = 0.0200$) at P150. The number of diffuse plaques is significantly higher in the neocortex at P90 in tgCRND8 mice (0.4 ± 0.05) compared to tgCRND8/tgDimer mice (0.2 ± 0.05 ; $p = 0.0346$). At P150, the number of diffuse plaques is significantly higher in both brain regions of the tgCRND8 mice (1.1 ± 0.1 , 0.9 ± 0.2) compared to the tgCRND8/tgDimer mice (0.4 ± 0.1 , 0.3 ± 0.1 ; $p = 0.0013$ and $p = 0.0073$, respectively). (C) The size of the core and diffuse plaques (in μ m²) in the neocortex and hippocampus are not different between the groups.

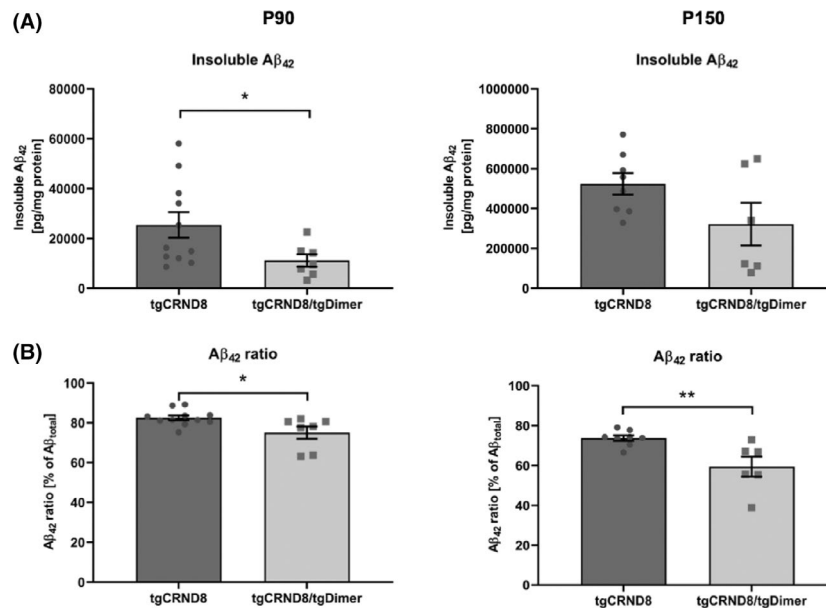


FIGURE 2 Differences in insoluble Aβ₄₂ levels and Aβ ratio between tgCRND8 and tgCRND8/tgDimer mice. (A) The level of insoluble Aβ₄₂ is higher in tgCRND8 mice (25,392 ± 5,149 pg/mg protein) compared to tgCRND8/tgDimer mice (11,138 ± 2,501 pg/mg protein, $p = 0.0441$) at P90. At P150, the insoluble Aβ₄₂ is also higher in tgCRND8 mice (523,455 ± 53,885 pg/mg protein) compared to tgCRND8/tgDimer mice (321,280 ± 106,856 pg/mg protein), although not reaching statistical significance ($p = 0.1812$). (B) The Aβ₄₂/total Aβ ratio is significantly higher in the tgCRND8 mice (P90: 82.5 ± 1.2%; P150: 73.7 ± 1.4%) versus tgCRND8/tgDimer (P90: 75.1 ± 3.1%; P150: 59.5 ± 5.0%) mice at both ages ($p = 0.0154$ and $p = 0.0081$ respectively).

of the haPrP promoter-driven hAPP₆₉₅(Swe/Ind) gene (Figure S1A), or Thy1 promoter-driven hAPP₇₅₁(Swe/Aβ-S8C) gene (Figure S1B) did not differ between the tgCRND8/tgDimer and tgCRND8 mice, respectively, or between the tgCRND8/tgDimer and tgDimer mice, respectively.

The influence of the Aβ-S8C dimers on plaque formation was assessed by quantifying dense or core plaques. Dense plaques are fibrillar deposits of Aβ, that show all the classical properties of amyloid including β-sheet secondary structure and dystrophic neurites surrounding the plaques, and diffuse plaques are amorphous Aβ deposits – an antecedent stage of core plaques (20). At the age of 90 and 150 days, both the tgCRND8 and tgCRND8/tgDimer mice showed Aβ plaques (Figure 1A). We quantified both Aβ core and diffuse plaques by measuring the number (per mm²) and size (in μm²) of plaques in coronal brain sections of tgCRND8 and tgCRND8/tgDimer mice at P90 and P150 (Figure 1A). In comparison to tgCRND8/tgDimer mice, tgCRND8 mice had significantly more Aβ core and diffuse plaques at P90 only in the earlier affected neocortex but not yet in the hippocampus (Figure 1B; $p = 0.0268$, $p = 0.0346$, $p = 0.0566$ and $p = 0.2638$, respectively). Later on, at P150, this difference also became detectable in the hippocampus (Figure 1B; $p = 0.0127$, $p = 0.0013$, $p = 0.0200$ and $p = 0.0073$ respectively). However, the average size of the plaques was not different between the groups (Figure 1C).

Insoluble Aβ₄₀ and Aβ₄₂ peptides from brain homogenates of tgCRND8/tgDimer and tgCRND8 mice at P90 and P150 were obtained via a four-step fractionation protocol (Figure S2) and quantified by ELISA. All concentrations were normalized using the total

protein concentration of the starting 10% brain homogenate. The level of insoluble Aβ₄₂ was significantly higher in tgCRND8 mice at P90 (25,392 ± 5,149 pg/mg protein) compared to tgCRND8/tgDimer mice (11,138 ± 2,501 pg/mg protein, Figure 2A $p = 0.0441$). The level of insoluble Aβ₄₂ at P150 in tgCRND8 mice (523,455 ± 53,885 pg/mg protein) was also higher as in the tgCRND8/tgDimer mice (321,280 ± 106,856 pg/mg protein) but failed statistical significance ($p = 0.1812$).

The Swedish mutation of APP does not change the Aβ₄₂/total Aβ ratio compared to wild-type APP. Consistently, we observed a ratio of 20% Aβ₄₂/total Aβ in tgDimer mice, which did not significantly change throughout the lifespan and was similar to wild-type mice (14), which indicates no accumulation of Aβ and especially Aβ₄₂. The Indiana mutation of APP in tgCRND8 mice, by contrast, markedly increased the generation of Aβ₄₂ and led to an average ratio of about 80% Aβ₄₂/total Aβ in the insoluble Aβ fraction derived from tgCRND8 similar to previous findings in other AD animal models (16,21). In tgCRND8/tgDimer mice, we detected a significant lower ratio of Aβ₄₂/total Aβ (P90: 75.1 ± 3.1%; P150: 59.5 ± 5.0) compared to tgCRND8 mice (P90: 82.5 ± 1.2; P150: 73.7 ± 1.4; Figure 2B $p = 0.0154$ and $p = 0.0080$). We did not observe significant amounts of other Aβ oligomer species in the brains of these mice (Figure S3).

Next, we analysed whether we could observe a correlation between Aβ plaque load and the concentrations of insoluble Aβ₄₂. At P90, there was a trend towards a positive correlation between the levels of insoluble Aβ₄₂ and the numbers of plaques in tgCRND8 mice (Figure S4, $p = 0.0856$) consistent with the idea that Aβ₄₂ is the most aggregation-prone Aβ species initiating seeding. Interestingly,

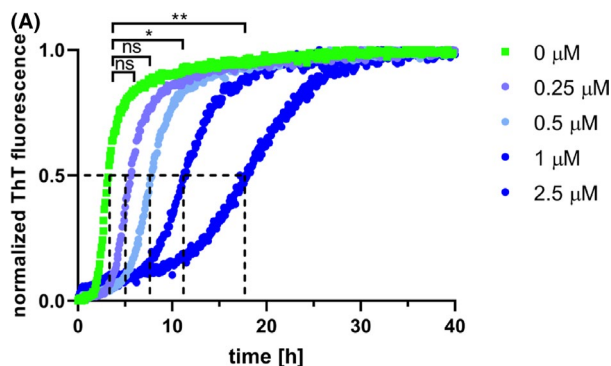


FIGURE 3 Effect of $A\beta_{42}$ -S8C dimers on $A\beta_{42}$ aggregation assay. $A\beta_{42}$ -S8C dimers added in various concentrations to $A\beta_{42}$ inhibit fibril formation. The half-time (defined as the time to reach 50% of maximum fluorescence) of 5 μM $A\beta_{42}$ without the addition of $A\beta_{42}$ -S8C is $3.2 \text{ h} \pm 0.1 \text{ h}$. At concentrations of 0.25 and 0.5 μM of $A\beta_{42}$ -S8C dimers (concentration given as monomer equivalents), a slight shift of the curve to the right is observed with an increase in aggregation half-time ($5.8 \text{ h} \pm 0.2 \text{ h}$; $7.7 \text{ h} \pm 0.3 \text{ h}$, not significant). The addition of higher concentrations, 1 μM and 2.5 μM $A\beta_{42}$ -S8C, results in a significant increase in the aggregation half-time (normalized data, one-way ANOVA, $11.3 \text{ h} \pm 0.5 \text{ h}$; $p = 0.0164$, and $17.9 \text{ h} \pm 1.2 \text{ h}$; $p = 0.0005$ respectively).

this correlation vanished later on, at P150 (Figure S4), possibly, as discussed by Burgold *et al.* (22) due to the fact that in the late “saturation phase” of plaque genesis *in vivo*, $A\beta$ is mainly added to existing plaques and does not reach the critical concentration for new nucleating seeds.

In contrast, in the case of tgCRND8/tgDimer mice, while there was no correlation between the number of plaques and $A\beta_{42}$ levels at P90, a significant positive correlation was present later, at P150 (Figure S5, $p = 0.0382$). This shift of a correlation between $A\beta_{42}$ level and plaques to older age is likely to be a consequence of decreased baseline $A\beta_{42}$ levels, reaching the saturation threshold later. Of note, despite the differences in the plaque burden, the level of neuroinflammation indicated by microgliosis or astrogliosis was similar in tgCRND8 versus tgCRND8/tgDimer mice (Figure S6).

The results here suggest that the presence of $A\beta$ -S8C dimers slows down the formation of new $A\beta$ plaques. An explanation for this observation is that the introduction of the disulfide cross-link causes steric hindrance for the dimeric $A\beta$ -S8C to form fibrils. The $A\beta$ -S8C dimer adopts a rather rigid conformation, which is different from the monomeric and oligomeric forms (13,23). As a result, the $A\beta$ -S8C dimer in the tgDimer is not prone to seed nucleation, as has been shown by molecular modelling and the fact that they do not develop plaques during their lifetime (13,23).

In order to corroborate the effect of $A\beta$ -S8C dimers on amyloid fibril formation *in vitro*, we dimerized synthetic $A\beta_{42}$ -S8C by letting it incubate in 50 mM HEPES NaOH pH 7.6 at 37°C with 450 rpm shaking. After 4 h, dimerization was complete (Figure S7), and the $A\beta$ -S8C dimer fraction was purified and collected via RP-HPLC and prepared for aggregation assays.

In a ThT assay, we added various concentrations of synthetic $A\beta_{42}$ -S8C dimers to wild-type $A\beta_{42}$. Without $A\beta_{42}$ -S8C dimers, $A\beta_{42}$ fibril formation was achieved with a half-time (defined as time to reach 50% of maximum fluorescence) of $3.2 \text{ h} \pm 0.1 \text{ h}$ (Figure 3). Addition of $A\beta_{42}$ -S8C dimers at a dose of 0.25 μM and 0.5 μM , increased the half-time of fibril formation in dose-dependent manner ($5.8 \text{ h} \pm 0.2 \text{ h}$ and $7.7 \text{ h} \pm 0.3 \text{ h}$, Figure 3, not significant). Addition of higher concentrations of $A\beta$ -S8C dimers: 1 μM and 2.5 μM $A\beta$ -S8C dimers, resulted in a more pronounced increased half-time ($11.3 \text{ h} \pm 0.5 \text{ h}$ and $17.9 \text{ h} \pm 1.2 \text{ h}$, Figure 3, normalized data, one-way ANOVA, $p = 0.0164$, $p = 0.0005$ respectively).

DISCUSSION

Our findings are remarkable in two ways: first, they show that $A\beta$ dimers, the $A\beta$ oligomer species best definable and likely most abundant in brains of AD patients (24), are able to inhibit $A\beta$ seeding, and second, that $A\beta$ plaque seeding and growth follow different dynamics. How could the discrepancy of seeding and growth be instated in molecular terms? Our previous molecular dynamics simulations demonstrated the inability of $A\beta$ -S8C dimers to form nuclei (13) (explaining the absence of $A\beta$ plaques in the tgDimer mouse), yet, their fundamental ability to associate with existing wild-type $A\beta$ plaque nuclei (14). The formation of wild-type $A\beta$ nuclei (= seeds) is fundamentally different from their growth, since the former is thermodynamically unfavourable, whereas the latter is thermodynamically favourable (25). Once the nucleus has formed, further addition of monomers becomes thermodynamically favourable because monomers contact the growing polymer at multiple sites which results in rapid growth. It is conceivable that $A\beta$ -S8C dimers intercept nucleation, thereby blocking growth, more efficiently in the initial stages of seeding when the nucleus or its precursor are unstable (25). In addition, $A\beta$ plaque surface area increases by an order of two relative to their radius, and thus disruptive effect of the $A\beta$ dimer is more efficient when the overall $A\beta$ plaque surface area is smaller in early stages rather than in late stages of plaque growth.

Our *in vivo* and *in vitro* data are also supported by findings where a single-chain dimeric variant of $A\beta_{40}$, with two $A\beta_{40}$ units connected via a flexible glycine-serine-rich linker, readily formed globular oligomers and curvilinear fibrils (12). Adding this $A\beta$ dimer species to $A\beta$ monomers progressively slowed rigid fibril (RF) formation, which was evident in the increasing RF lag periods. It was argued that the formation of metastable oligomers therefore alters RF nucleation (12). Similarly, $A\beta$ -S8C dimers may interfere with fibril formation, by inhibiting nucleation, which would be an explanation for the increased half-time of the aggregation curves in the ThT assay by addition of $A\beta_{42}$ -S8C dimers.

The well-known intersubject heterogeneity of $A\beta$ plaque load (1-3) likely has multiple origins. For example, it has been suggested that it may be related to different $A\beta$ prion conformers that reliably replicate within one individual brain, but that are not similar between

two or more AD brains leading to a low intrasubject variability but a high intersubject variability of A β conformers (26) that may, to some degree, correspond to different numbers of plaque formation. The contribution of microglia or myeloid cells to A β plaque load has also been emphasized (27). With this study, we add evidence for the inhibiting effect of A β dimers as a cause for A β plaque load heterogeneity, if it is assumed that the equilibrium between insoluble A β seeds and the simultaneously available amount of A β dimers is highly variable between individual AD cases and subject to the influence of a multitude of factors.

We demonstrated that two neurotoxic A β species, soluble A β dimers and insoluble A β , can have opposing effects on a classical diagnostic feature of AD, the abundance of A β plaques. Our insights indicate that correlating the clinical severity of AD defined by cognitive deficits with a mere morphological phenotype, A β plaque numbers, may insufficiently reflect the underlying equilibrium of functionally active, neurotoxic A β species. Current clinical diagnostics not distinguishing different A β species like A β positron emission tomography or the detection of whole A β species levels in cerebrospinal fluids are therefore in danger of picking misleading biological variables. A more fine-grained A β species diagnostics may therefore be beneficial, including for predicting the value of A β -targeted pharmacotherapies.

In conclusion, we have demonstrated that A β oligomers – here A β -S8C dimers – are able to decrease A β plaque seeding *in vivo* and *in vitro* and are a contributing factor to the clinical heterogeneity of A β plaque load in individuals suffering from AD or even cognitively unimpaired controls.

ACKNOWLEDGEMENT

This work was supported by a grant from the DFG (KO 1679/10-1) and BMBF (01GQ1422A) to C.K. and from the Russian Science Foundation (RSF) (project no. 20-64-46027) to L.G. for A β -S8C dimer preparations and ThT aggregation assays.

CONFLICT OF INTEREST

All authors declare no conflict of interest.

AUTHOR CONTRIBUTIONS

K.K., C.K., A.H. and A.M.-S. conceived and outlined the experiments. C.K., K.K., A.M.-S., L.G., A.H. and E.v.G. planned and supervised experiments. E.v.G., A.H. and L.G. performed experiments, collected and analysed data. All authors participated in writing and correcting the manuscript.

ETHICAL APPROVAL

Animal experiments were performed in accordance with the German Animal Protection Law and were authorized by local authorities (LANUV NRW, Germany).

PEER REVIEW

The peer review history for this article is available at <https://publons.com/publon/10.1111/nan.12685>.

DATA AVAILABILITY STATEMENT

All original data will be made available upon reasonable request.

ORCID

Lothar Gremer  <https://orcid.org/0000-0001-7065-5027>

Kathy Keyvani  <https://orcid.org/0000-0003-2558-5159>

Carsten Korth  <https://orcid.org/0000-0003-1503-1822>

REFERENCES

1. Lam B, Masellis M, Freedman M, Stuss DT, Black SE. Clinical, imaging, and pathological heterogeneity of the Alzheimer's disease syndrome. *Alzheimer's research & therapy*. 2013; 5(1): 1.
2. Bird TD, Sumi SM, Nemens EJ, et al. Phenotypic heterogeneity in familial Alzheimer's disease: a study of 24 kindreds. *Ann Neurol*. 1989; 25(1): 12-25.
3. Cupidi C, Capobianco R, Goffredo D, et al. Neocortical variation of Abeta load in fully expressed, pure Alzheimer's disease. *Journal of Alzheimer's disease: JAD*. 2010; 19(1): 57-68.
4. Zhang S, Smailagic N, Hyde C, et al. (11)C-PIB-PET for the early diagnosis of Alzheimer's disease dementia and other dementias in people with mild cognitive impairment (MCI). *Cochrane Database Syst Rev*. 2014;7:CD010386.
5. McLean CA, Cherny RA, Fraser FW, et al. Soluble pool of Abeta amyloid as a determinant of severity of neurodegeneration in Alzheimer's disease. *Ann Neurol*. 1999; 46(6): 860-866.
6. Haass C, Selkoe DJ. Soluble protein oligomers in neurodegeneration: lessons from the Alzheimer's amyloid beta-peptide. *Nature Rev Mol Cell Biol*. 2007; 8(2): 101-112.
7. Lee J, Culyba EK, Powers ET, Kelly JW. Amyloid-beta forms fibrils by nucleated conformational conversion of oligomers. *Nat Chem Biol*. 2011; 7(9): 602-609.
8. Gaspar RC, Villarreal SA, Bowles N, Hepler RW, Joyce JG, Shughrue PJ. Oligomers of beta-amyloid are sequestered into and seed new plaques in the brains of an AD mouse model. *Exp Neurol*. 2010; 223(2): 394-400.
9. Koffie RM, Meyer-Luehmann M, Hashimoto T, et al. Oligomeric amyloid beta associates with postsynaptic densities and correlates with excitatory synapse loss near senile plaques. *Proc Natl Acad Sci U S A*. 2009; 106(10): 4012-4017.
10. Yamaguchi T, Yagi H, Goto Y, Matsuzaki K, Hoshino M. A disulfide-linked amyloid-beta peptide dimer forms a protofibril-like oligomer through a distinct pathway from amyloid fibril formation. *Biochemistry*. 2010; 49(33): 7100-7107.
11. Sandberg A, Luheshi LM, Sollvander S, et al. Stabilization of neurotoxic Alzheimer amyloid-beta oligomers by protein engineering. *Proc Natl Acad Sci U S A*. 2010; 107(35): 15595-15600.
12. Hasecke F, Miti T, Perez C, et al. Origin of metastable oligomers and their effects on amyloid fibril self-assembly. *Chemical science*. 2018; 9(27): 5937-5948.
13. Muller-Schiffmann A, Andreyeva A, Horn AH, Gottmann K, Korth C, Sticht H. Molecular engineering of a secreted, highly homogeneous, and neurotoxic abeta dimer. *ACS Chem Neurosci*. 2011; 2(5): 242-248.
14. Muller-Schiffmann A, Herring A, Abdel-Hafiz L, et al. Amyloid-beta dimers in the absence of plaque pathology impair learning and synaptic plasticity. *Brain*. 2016; 139(Pt 2): 509-525.
15. Abdel-Hafiz L, Muller-Schiffmann A, Korth C, et al. Abeta dimers induce behavioral and neurochemical deficits of relevance to early Alzheimer's disease. *Neurobiol Aging*. 2018; 69: 1-9.
16. Chishti MA, Yang D-S, Janus C, et al. Early-onset amyloid deposition and cognitive deficits in transgenic mice expressing a double mutant form of amyloid precursor protein 695. *J Biol Chem*. 2001; 276(24): 21562-21570.

17. Müller-Schiffmann A, März-Berberich J, Andreyeva A, et al. Combining independent drug classes into superior, synergistically acting hybrid molecules. *Angew Chem*. 2010; 49(46): 8743-8746.
18. Sisodia SS, Koo EH, Hoffman PN, Perry G, Price DL. Identification and transport of full-length amyloid precursor proteins in rat peripheral nervous system. *J Neurosci*. 1993; 13(7): 3136-3142.
19. Kawarabayashi T, Younkin LH, Saido TC, Shoji M, Ashe KH, Younkin SG. Age-dependent changes in brain, CSF, and plasma amyloid (beta) protein in the Tg2576 transgenic mouse model of Alzheimer's disease. *J Neurosci*. 2001; 21(2): 372-381.
20. Rak M, Del Bigio MR, Mai S, Westaway D, Gough K. Dense-core and diffuse Abeta plaques in TgCRND8 mice studied with synchrotron FTIR microspectroscopy. *Biopolymers*. 2007; 87(4): 207-217.
21. Sturchler-Pierrat C, Abramowski D, Duke M, et al. Two amyloid precursor protein transgenic mouse models with Alzheimer disease-like pathology. *Proc Natl Acad Sci U S A*. 1997; 94(24): 13287-13292.
22. Burgold S, Filser S, Dorostkar MM, Schmidt B, Herms J. In vivo imaging reveals sigmoidal growth kinetic of beta-amyloid plaques. *Acta Neuropathol Commun*. 2014; 2: 30.
23. Horn AH, Sticht H. Amyloid-beta42 oligomer structures from fibrils: a systematic molecular dynamics study. *J Phys Chem B*. 2010; 114(6): 2219-2226.
24. Shankar GM, Li S, Mehta TH, et al. Amyloid-beta protein dimers isolated directly from Alzheimer's brains impair synaptic plasticity and memory. *Nat Med*. 2008; 14(8): 837-842.
25. Jarrett JT, Lansbury PT Jr. Seeding "one-dimensional crystallization" of amyloid: a pathogenic mechanism in Alzheimer's disease and scrapie? *Cell*. 1993; 73(6): 1055-1058.
26. Condello C, Lemmin T, Stohr J, et al. Structural heterogeneity and intersubject variability of Abeta in familial and sporadic Alzheimer's disease. *Proc Natl Acad Sci U S A*. 2018; 115(4): E782-E791.
27. Prokop S, Miller KR, Drost N, et al. Impact of peripheral myeloid cells on amyloid-beta pathology in Alzheimer's disease-like mice. *J Exp Med*. 2015; 212(11): 1811-1818.

SUPPORTING INFORMATION

Additional supporting information may be found online in the Supporting Information section.

How to cite this article: Gerresheim EF, Herring A, Gremer L, Müller-Schiffmann A, Keyvani K, Korth C. The interaction of insoluble Amyloid- β with soluble Amyloid- β dimers decreases Amyloid- β plaque numbers. *Neuropathol Appl Neurobiol*. 2021;47:603-610. <https://doi.org/10.1111/nan.12685>